# Combining Model-based and Data-based approaches for online predictions of human trajectories

Aymeric Orhan, Dorian Verdel, Olivier Bruneau, Franck Geffard, Bastien Berret

# Combining Model-based and Data-based approaches for online predictions of human trajectories

Aymeric Orhan, Dorian Verdel, Olivier Bruneau, Franck Geffard and Bastien Berret

***Abstract*— Accurately predicting human movement trajectories is of critical interest in multiple fields, including human-exoskeleton interaction. In general, such predictions can be obtained from model-based approaches (e.g., optimal control theory) or from data-driven approaches (e.g., learning from human demonstrations). Data-driven methods generally require numerous demonstrations but avoid the computational burden of model-based methods. In this paper, we introduce a hybrid method mixing the strengths of these two approaches to enable the prediction of human trajectories in a receding-horizon fashion when the number of actual demonstrations is very limited. First, we propose to use the stochastic optimal feedforward-feedback control framework to generate a large set of humanlike trajectories, including their variability. Second, we used the probabilistic movement primitives (ProMPs) framework to learn the distribution of these synthetic trajectories and make online predictions about the upcoming human trajectories from the observation of past movement data. Here, we evaluated our hybrid method on an existing data set composed of arm reaching movements in a parasagittal plane. Overall, our method proves to be advantageous when generalization is needed and demonstrations are lacking, such as in novel targets scenarios. The introduced method shows promise to efficiently predict realistic human trajectories on a given time horizon, even when limited or no human demonstration is available for the task at hand.**

## I. Introduction

Exoskeletons show great promise as devices for physically assisting humans in various tasks, in particular for health-related applications such as neurorehabilitation [1] and preventing musculoskeletal disorders in workers [2]. In order to achieve this goal, it is typically necessary to predict the intended human movements to design assistive controllers complying with both human motor control principles and the task at hand [3], [4].

On the one hand, the detection of human motion intent at a high level is often achieved using classifiers based on physiological recordings, such as electroencephalography (EEG) [5], electromyography (EMG) [6], or gaze [7]. However, such classification methods only provide abstract intents, such as future direction or target, which does not allow to optimize the assistance level provided by the exoskeleton during the whole movement. On the other hand, when the upcoming trajectory is not predefined (in contrast with [8], [9]), its prediction is usually achieved either by regressing from physiological recordings such as EMG in continuous time [10], [11] or from kinematic recordings as commonly done in learning-by-demonstration approaches [12].

Overall, kinematic-based learning methods have undergone more extensive field testing and are more likely to be successfully integrated into exoskeletons in the coming years. Indeed, multiple approaches ranging from pioneer dynamic movement primitives [13] to unsupervised learning of human trajectories [14], have already proven to be powerful tools to predict human trajectories. In the present paper, we focus on probabilistic movement primitives (ProMPs) because they allow to represent the distribution of human trajectories in a compact form and provide efficient online prediction tools [15]. Furthermore, they have proven to be particularly adapted to predict trajectories in the context of human-exoskeleton interaction [16]. However, as all learning by demonstration techniques, collecting a comprehensive dataset to train ProMPs can be a tedious task. Here, we propose to address this training issue by leveraging recent advances in human motor control, which enable to generate large amounts of humanlike trajectories from a model-based approach.

Specifically, the average human motor behavior has been shown to be well described by optimal control models minimizing criteria such as effort [17], smoothness [18], variance [19], time [20], or a compromise of these criteria [21]. Consequently, for a given set of human trajectories, one can identify a cost function to minimize that will accurately represent the average of the provided data using inverse optimal control [21]. However, human movement have an inherent variability resulting mostly from the noise in the sensorimotor system [22] so that stochastic optimal control (OC) has become the main framework to model human motor control [23]. Unfortunately, such methods are often computationally demanding, which makes their online implementation difficult. Here, we focus on an approximate stochastic optimal control framework that represents movement planning and feedback control under uncertainties as a stochastic optimal feedforward-feedback control (SFFC) problem [24]. Interestingly, this approach has been shown to be able to replicate the characteristics of human trajectories (including their variability) while remaining easily applicable

Dorian Verdel is with the Human Robotics Group, Department of Bioengineering, Imperial College of Science, Technology and Medicine, W12 0BZ London, United-Kingdom

Olivier Bruneau is with the LURPA, Mechanical Engineering Department, ENS Paris-Saclay, Université Paris-Saclay, 91190 Gif-sur-Yvette, France.

Bastien Berret is with the CIAMS, Sport Sciences Department, Université Paris-Saclay, Orsay, France, the CIAMS, Université d'Orléans, Orléans, France.

Franck Geffard and Aymeric Orhan are with the CEA, List, Université Paris-Saclay, Palaiseau, France

This work is supported in part by the French National Agency for Research (grant ANR-19-CE33-0009)

Correspondence should be adressed to Aymeric Orhan: aymeric.orhan@cea.fr

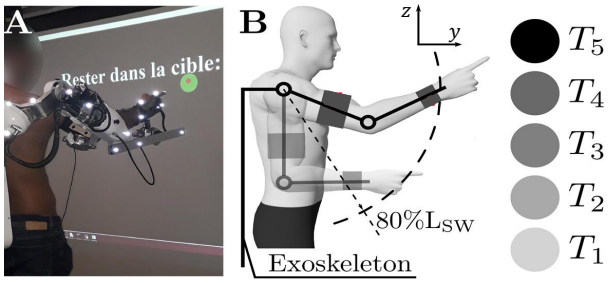


Fig. 1. Experimental setup. Subjects performed movements from the starting position (shaded) towards one of the targets positioned in the parasagittal plane. The targets were displayed on a screen (in green in the figure) in front of the subject. The subjects were given visual feedback with regard to their current index finger pointing position with a red cursor.

to nonlinear musculoskeletal dynamics. Hence, they could be used to generate large artificial sets of humanlike trajectories based on state-of-the-art knowledge in human motor control, without needing to record human movements. In machine learning, this approach belongs to the generation of synthetic data. We hypothesize that this hybrid approach can be viable and outperform a pure data-driven approach when generalization is needed (e.g., new tasks for which no demonstration is available). To test this premise we first generate a set of humanlike trajectories using SFFC to train ProMPs. Then, the quality of the predictions of the trained ProMPs is assessed against a pre-existing set of 2-degrees of freedom arm reaching movements in a parasagittal plane [25].

## II. Materials and Methods

In this section, we first describe the dataset used to train the ProMPs and test the proposed hybrid model. The metric used for this evaluation is also presented. Then, we successively introduce the human arm's model, review the method of ProMPs and present the OC method to generate humanlike trajectories.

### A. Dataset

As stated in the introduction, the dataset used throughout this study is the one described in [25]. We briefly summarize the main characteristics below.

**Participants.** A total of 14 participants (3 females), took part in the experiment. The participants, with a mean age of 26.33±2.93 years, mean height of 1.76±0.05m, and mean weight of 72.87±6.43kg, were healthy, right-handed adults without any known neurological disorders or injuries that could have affected the experiment. Written informed consent was obtained from all participants in accordance with the Helsinki declaration, and the protocol was approved by the local ethical committee for research (CER-Paris-Saclay-2021-048).

**Task.** The task involved executing arm reaching movements in a parasagittal plane $(y, z)$ towards five targets displayed on a screen in front of the subjects as shown in Fig. 1. A display on the screen indicated to the participant the validity of the reference position, characterized by the arm being vertical, forming a 90° angle with the elbow, and extending the index finger. Subsequently, a target, depicted as a blue disk was displayed in front of the participant. A trial was deemed valid if the participant pointed at the target with the arm extended. In particular, it was ensured that the distance from the shoulder to wrist was at least 80% of the combined length of the arm and forearm (LSW). The target turned green when the trial was validated. 24 movements per target per subject were performed in a random order.

**Data Collection.** The reaching task was performed while wearing a backdrivable robotic exoskeleton for the upper limb (ABLE, [26], [27]). This exoskeleton features four active joints, three replicating the human gleno-humeral joint and one emulating human elbow flexion/extension. To maximize transparency and mitigate unwanted interaction efforts, two passive rotations and a passive translation were incorporated at the forearm level, aligning with prior works from [28], [29]. Movements were measured using the internal encoders of the exoskeleton worn by participants at a frequency of 1 kHz, then down-sampled to 100 Hz. We recorded the joint positions along each movements and filtered possible initial and final waiting period where both joints were immobile.

**Comparison metric.** Our goal is to predict the upcoming arm trajectory of a user on some receding horizon of length $h \in \mathbb{N}^\star$, in a discrete time setting. To evaluate our predictions, we measured the average deviation between the recorded experimental trajectory and the predicted one over the chosen horizon. Let us denote by $t \in \{0, 1, \dots, T\}$ the current time within an experimental trajectory of length $T+1$. The corresponding experimental position of the endpoint is denoted by $\boldsymbol{p}_t^{\text{exp}} = [\boldsymbol{y}_t, \boldsymbol{z}_t]^\top$. At any time $t$, we build a prediction about the upcoming trajectory, denoted by $\boldsymbol{p}_{s|t}^{\text{pred}}$, which is defined for times $s \in \{t, \dots, t + \Delta\}$ where $\Delta = \min(h, T - t)$. Then, the prediction error at time $t$, denoted by $e_t$, was computed as follows:

$$e_t = \frac{1}{\Delta} \sum_{s=t}^{t+\Delta} \|\boldsymbol{p}_s^{\text{exp}} - \boldsymbol{p}_{s|t}^{\text{pred}}\|. \tag{1}$$

The error is defined on a receding horizon because updating predictions during the movement has been shown to translate into a more effective assistance compared to using a monolithic prediction [16]. As such, the error on the receding horizon of length $\Delta + 1$ reflects the prediction error with the most recent knowledge of the endpoint position. In this paper, we evaluated our predictions on horizons of lengths $h = 5$, $h = 10$ and $h = 20$ (i.e., from 50 ms to 200 ms), so as to match the frequency of prediction update in the literature [16] and assess the criticity of the prediction rate. Longer horizons were not considered because the movements under consideration lasted less than 1.5 s on average.

### B. Arm's model

The human arm is modelled as a two-joints rigid body with the shoulder and elbow flexion/extension angles respectively

denoted as $\boldsymbol{q}_1$ and $\boldsymbol{q}_2$. Lengths, masses and centers of gravity of the upper-arm and forearm are respectively denoted as $l_1, m_1, I_1$ and $l_2, m_2, I_2$ with $L = l_1 + l_2$ the arm length. The arm dynamics were formulated using Lagrangian mechanics as follows:

$$\boldsymbol{\tau} = \mathcal{M}(\boldsymbol{q})\ddot{\boldsymbol{q}} + \mathcal{C}(\boldsymbol{q}, \dot{\boldsymbol{q}})\dot{\boldsymbol{q}} + \mathcal{G}(\boldsymbol{q}) + \mathcal{F}\dot{\boldsymbol{q}}, \tag{2}$$

where $\boldsymbol{\tau} = [\tau_1, \tau_2]^\top$ and $\boldsymbol{q} = [q_1, q_2]^\top$ denote the torque and joint angle vectors, and where a *dot* above a variable corresponds to its time derivative. $\mathcal{M}, \mathcal{C}, \mathcal{G}$ and $\mathcal{F}$ are respectively the inertia matrix, the Coriolis/centripetal matrix, the gravitational vector and the friction (damping) matrix.

Furthermore, the smooth production of torque through muscle contractions was accounted for by considering that torque is a twice-differentiable function of time as in [21]:

$$\dddot{\boldsymbol{\tau}} = \boldsymbol{u}. \tag{3}$$

In this model, it is assumed that the brain directly regulates the joint torque second time derivative, thus simplifying the system. It would be straightforward to consider other types of muscle dynamics (see [11] for examples) but this is not critical to the present study. Equations (2)-(3) can be rewritten in state-space form by defining the state vector $\boldsymbol{x} = [\boldsymbol{q}^\top, \dot{\boldsymbol{q}}^\top, \boldsymbol{\tau}^\top, \dot{\boldsymbol{\tau}}^\top]^\top$.

### C. Probabilistic Movement Primitives

In the present paper, we used Probabilistic Movement Primitives to perform predictions about upcoming human movements. ProMPs is a data-driven method that can learn a distribution over discrete-time trajectories [15]. It is data-driven in the sense that demonstrations are needed in order to learn such a distribution. Then, predictions about the upcoming trajectory can be obtained at low computational cost by conditioning the distribution with an observation. Below, we briefly describe the ProMPs method in our context, the reader is deferred to [15] and references therein for full details.

*1) Encoding demonstrations:* ProMPs encode trajectories using basis functions. Here, we used Gaussian basis functions as is common practice for discrete point-to-point movements formulated in the joint space [15]. Let $\boldsymbol{\Gamma}_t = [q_{1,t}, \dot{q}_{1,t}, q_{2,t}, \dot{q}_{2,t}]^\top$ be the arm's joints position and velocity at time $t \in \{0, 1, \dots, T\}$. The full trajectory can be represented by vertical concatenation as the vector $\boldsymbol{\Gamma}_{0:T} = [\boldsymbol{\Gamma}_0^\top, \cdots, \boldsymbol{\Gamma}_T^\top]^\top \in \mathbb{R}^{4(T+1)}$. Let $\boldsymbol{\Phi}_{i,t} = [\phi_{i,t}, \dot{\phi}_{i,t}] \in \mathbb{R}^{n \times 2}$ denote the basis matrix for a single joint position and velocity $q_{i,t}$ and $\dot{q}_{i,t}$,with $i = 1$ and 2 for the shoulder and elbow respectively, and $n$ a parameter defining the number of Gaussian basis functions. These matrices of basis functions at time $t$ are concatenated in a block diagonal matrix $\boldsymbol{\Psi}_t = \text{blkdiag}(\boldsymbol{\Phi}_{1,t}^\top, \boldsymbol{\Phi}_{2,t}^\top) \in \mathbb{R}^{4 \times 2n}$. This matrix is then extended to include all time steps by vertical concatenation $\boldsymbol{\Psi}_{0:T} = [\boldsymbol{\Psi}_0^\top \cdots \boldsymbol{\Psi}_T^\top]^\top \in \mathbb{R}^{4(T+1) \times 2n}$. Finally, the joint space trajectory of the arm is represented via a $2n$-dimensional weight vector $\boldsymbol{w} \in \mathbb{R}^{2n}$, as follows:

$$\boldsymbol{\Gamma}_t = \boldsymbol{\Psi}_t \boldsymbol{w} + \boldsymbol{\epsilon}_\Gamma \tag{4}$$

with $\boldsymbol{\epsilon}_\Gamma \sim \mathcal{N}(0, \boldsymbol{\Sigma}_\Gamma)$ i.i.d. Gaussian noise. We can then express the probability of observing a trajectory $\boldsymbol{\Gamma}_{0:T}$ using the weight vector $\boldsymbol{w}$:

$$p(\boldsymbol{\Gamma}_{0:T}|\boldsymbol{w}) = \prod_{t=0}^{T} \mathcal{N}(\boldsymbol{\Gamma}_t|\boldsymbol{\Psi}_t \boldsymbol{w}, \boldsymbol{\Sigma}_\Gamma). \tag{5}$$

The weight vector associated with each demonstrated trajectory is estimated using a regression method. In this work we used the ordinary least square (OLS) method as in [16], here written for the trajectory $\boldsymbol{\Gamma}_{0:T}$:

$$\boldsymbol{w} = (\boldsymbol{\Psi}_{0:T}^\top \boldsymbol{\Psi}_{0:T} + \lambda \boldsymbol{I})^{-1} \boldsymbol{\Psi}_{0:T}^\top \boldsymbol{\Gamma}_{0:T} \tag{6}$$

with $\lambda = 10^{-2}$ a regularization parameter taken from [16].

As is common practice with motion primitives we introduced a phase parameter $\tau$ so as to enable temporal scaling and modulation. We simply defined the phase as normalized in this work (i.e. $\tau = t/(T+1)$). Basis functions are thus defined as depending on the phase of movement instead of time: $\boldsymbol{\Phi}_{i,t} = \boldsymbol{\Phi}_{i,\tau}$.

*2) Representation of variability:* Before being able to predict the upcoming trajectory from observations up to time $t$, one must capture the variability of human trajectories. To this aim, the weight vector is itself modelled as following a Gaussian distribution with $p(\boldsymbol{w}; \boldsymbol{\mu}_w, \boldsymbol{\Sigma}_w)$. Then, the mean and covariance parameters can be estimated from several demonstrations as follows:

$$\begin{aligned} \boldsymbol{\mu}_w &= \frac{1}{M} \sum_{i=1}^{M} \boldsymbol{w}_i, \\ \boldsymbol{\Sigma}_w &= \frac{1}{M-1} \sum_{i=1}^{M} (\boldsymbol{w}_i - \boldsymbol{\mu}_w)(\boldsymbol{w}_i - \boldsymbol{\mu}_w)^\top \end{aligned} \tag{7}$$

where $M$ is the number of demonstrations and $\boldsymbol{w}_i$ is the weight computed for the $i^{\text{th}}$ trajectory from (6).

*3) Trajectory prediction from observation:* An inference can then be obtained from an observation $\boldsymbol{\Lambda}_\tau^{\text{obs}} = \{\boldsymbol{\Gamma}_\tau^{\text{obs}}, \boldsymbol{\Sigma}_\Gamma^{\text{obs}}\}$ by adding it to our model and applying Bayes theorem, i.e. $p(\boldsymbol{w}|\boldsymbol{\Lambda}_\tau^{\text{obs}}) \propto \mathcal{N}(\boldsymbol{\Gamma}_\tau^{\text{obs}}|\boldsymbol{\Psi}_\tau \boldsymbol{w}, \boldsymbol{\Sigma}_\Gamma^{\text{obs}}) p(\boldsymbol{w})$. The distribution of $\boldsymbol{w}$ conditioned by the observation $\boldsymbol{\Lambda}_\tau^{\text{obs}}$ is Gaussian and given by the following mean and covariance:

$$\begin{aligned} \hat{\boldsymbol{\mu}}_w &= \boldsymbol{\mu}_w + \boldsymbol{\Sigma}_w \boldsymbol{\Psi}_\tau^\top \boldsymbol{S}_\tau (\boldsymbol{\Gamma}_\tau^{\text{obs}} - \boldsymbol{\Psi}_\tau \boldsymbol{\mu}_w), \\ \hat{\boldsymbol{\Sigma}}_w &= \boldsymbol{\Sigma}_w - \boldsymbol{\Sigma}_w \boldsymbol{\Psi}_\tau^\top \boldsymbol{S}_\tau \boldsymbol{\Psi}_\tau \boldsymbol{\Sigma}_w \end{aligned} \tag{8}$$

where $\boldsymbol{S}_\tau = (\boldsymbol{\Sigma}_\Gamma^{\text{obs}} + \boldsymbol{\Psi}_\tau \boldsymbol{\Sigma}_w \boldsymbol{\Psi}_\tau^\top)^{-1}$.

The prediction $\boldsymbol{\Gamma}_{0:T}^{\text{pred}}$ can then be computed by weighting the basis functions with the mean of this conditioned distribution:

$$\boldsymbol{\Gamma}_{0:T}^{\text{pred}} = \boldsymbol{\Psi}_{0:T} \hat{\boldsymbol{\mu}}_w. \tag{9}$$

This conditioning allows the ProMPs to predict trajectories that are not present in the training dataset. As such the predictions can be adapted to the center of a new target as shown in Fig. 5. We used this last point conditioning (LPC) feature when comparing the pure data-driven approach with our approach so as to compare the methods in scenarios with identical initial information. Finally, even though we

expressed the ProMPs in joint space, it should be noted that we can transfer predictions to the task space using forward kinematics.

### D. Optimal Control Framework

OC is a classical framework to synthetize humanlike optimal trajectories by minimizing a well-chosen cost function. If deterministic OC is able to capture the average trajectory, stochastic OC is the method of choice to capture the variability of human behavior. Here we used an approximate stochastic OC framework to generate humanlike trajectories. It is based on the following approach: (i) generate the mean behavior by solving a deterministic OC minimizing a composite cost function, as suggested by the motor control literature [21]; and (ii) generate the variability around this mean behavior by solving a locally-optimal stochastic OC of the linear-quadratic-Gaussian (LQG) type. This approach is classical in control theory and similar to the stochastic optimal feedforward-feedback (SFFC) framework introduced in [24].

*1) Optimal feedforward control:* To account for the average trajectory of human subjects, we first have to choose a suitable cost function, denoted by $C_{\text{ff}}$. Similar movements were studied in [21] using inverse optimal control, and it has been shown that a combination of smoothness (squared acceleration), effort (absolute work), and time allows to reproduce both their average path and duration, which is critical for efficient assistance [4]. The cost function for the feedforward OC problem was thus written as follows:

$$C_{\text{ff}} = \sum_{t=0}^{T} \alpha_1 \ddot{\boldsymbol{q}}^\top \ddot{\boldsymbol{q}} + \alpha_2 \left(|\dot{q}_{1,t}\tau_{1,t}| + |\dot{q}_{2,t}\tau_{2,t}|\right) + \frac{\alpha_3}{1+\zeta t} \quad (10)$$

where the weights $\alpha_i$, $i \in \{1,2,3\}$ define the trade-off between effort, smoothness and time. Let us define $\boldsymbol{\alpha} = [\alpha_1, \alpha_2, \alpha_3]^\top$. And where $\zeta$ is a parameter taken from [20] ($\zeta$=4.3).

In general, $\boldsymbol{\alpha}$ could be identified for each participant to account for individual preferences (i.e., individual path and speed). However, consistently with our approach, we adjusted the weights to reproduce the behavior of the average participant for all the simulations, which would allow to avoid the use of further demonstrations in practical implementation. We set $\boldsymbol{\alpha} = [0.1, 1, 5.6]^\top$.

The feedforward OC problem of Eq. 10 is then transformed into a nonlinear programming (NLP) problem with constraints before being solved using the open-source python software CasADi [30] with the IPOPT solver [31]. In order to reduce the computational cost and ensure the convergence of the NLP solver we initialized the problem with a minimal jerk initial guess [32]. A regularization term, quadratic in the control $\boldsymbol{u}$, was also added for numerical stability. To estimate the cost of time parameters, differently from [20], a direct optimization with Bobyqa [33] was used for optimizing $\alpha_3$ until we recover the average experimental duration.

In discrete time, the feedforward OC problem consists of finding an optimal control sequence $\bar{\boldsymbol{u}}_{0:T}$ corresponding to an optimal trajectory $\bar{\boldsymbol{x}}_{0:T}$ connecting an initial equilibrium state $\boldsymbol{x}_{\text{ini}}$ to a final equilibrium state $\boldsymbol{x}_{\text{end}}$, while minimizing the cost function $C_{\text{ff}}$.

To formulate the problem, one needs to express the state-space representation of the arm's dynamics in discrete time, which can be written as

$$\boldsymbol{x}_{t+1} = \boldsymbol{f}(\boldsymbol{x}_t, \boldsymbol{u}_t) \quad (11)$$

where the specific form of $\boldsymbol{f}$ depends on (2)-(3) and the choice of the discretization (e.g., Euler).

*2) Locally optimal feedback control:* Once a nominal motor plan $(\bar{\boldsymbol{u}}_{0:T}, \bar{\boldsymbol{x}}_{0:T})$ is obtained, one can consider the variability around it to generate an artificial dataset of humanlike trajectories on which we can train the ProMPs. This is achieved by considering the sensorimotor noise acting in the central nervous system. Below, we consider a local approximation using the nominal plan and formulate a linear-quadratic-Gaussian (LQG) problem.

Let us assume that sensorimotor system can be written as the following stochastic difference equation (e.g., after Euler–Maruyama's discretization):

$$\begin{aligned} \boldsymbol{x}_{t+1} &= \boldsymbol{f}(\boldsymbol{x}_t, \boldsymbol{u}_t) + \boldsymbol{G}(\boldsymbol{u}_t)\boldsymbol{\xi}_t \\ \boldsymbol{y}_t &= \boldsymbol{g}(\boldsymbol{x}_t) + \boldsymbol{\eta}_t \end{aligned} \quad (12)$$

where $\boldsymbol{x}_t$ denotes the stochastic state vector, $\boldsymbol{f}$ is the deterministic dynamics, $\boldsymbol{G}$ describes how motor noise affects the state, $\boldsymbol{y}_t$ is the sensory feedback and $\boldsymbol{g}$ is the output function. The terms $\boldsymbol{\xi}_t$ and $\boldsymbol{\eta}_t$ are i.i.d. zero-mean Gaussian random variables of appropriate dimensions, corresponding respectively to motor and observation noise.

Precisely, the matrix $\boldsymbol{G}$ was defined to capture the effects of both additive and multiplicative noise on the motor command, as follows:

$$\boldsymbol{G}(\boldsymbol{u}) = \begin{pmatrix} \multicolumn{4}{c}{\mathbf{0}_{6\text{x}4}} \\ \sigma_1 & \lambda_1 u_1 & 0 & 0 \\ 0 & 0 & \sigma_2 & \lambda_2 u_2 \end{pmatrix} \quad (13)$$

where $\boldsymbol{\sigma} = [\sigma_1, \sigma_2]^\top$ and $\boldsymbol{\lambda} = [\lambda_1, \lambda_2]^\top$ represent respectively the additive and multiplicative noise magnitudes.

Assuming that the system will remain in the vicinity of the planned control-trajectory pair thanks to the feedback control, we next linearized the above system around $(\bar{\boldsymbol{u}}_{0:T}, \bar{\boldsymbol{x}}_{0:T})$ to formulate a tractable LQG problem.

To this aim, let us define

$$\begin{aligned} &\delta\boldsymbol{x}_t = \boldsymbol{x}_t - \bar{\boldsymbol{x}}_t \quad , \quad \delta\boldsymbol{u}_t = \boldsymbol{u}_t - \bar{\boldsymbol{u}}_t \\ &\boldsymbol{A}_t = \frac{\partial \boldsymbol{f}}{\partial \boldsymbol{x}}_{|\bar{\boldsymbol{x}}_t, \bar{\boldsymbol{u}}_t}, \quad \boldsymbol{B}_t = \frac{\partial \boldsymbol{f}}{\partial \boldsymbol{u}}_{|\bar{\boldsymbol{x}}_t, \bar{\boldsymbol{u}}_t} \text{ and } \quad \boldsymbol{C}_t = \frac{\partial \boldsymbol{g}}{\partial \boldsymbol{x}}_{|\bar{\boldsymbol{x}}_t} \end{aligned} \quad (14)$$

If we denote $\boldsymbol{G}_t = \boldsymbol{G}(\bar{\boldsymbol{u}}_t)$, then after linearization around $\bar{\boldsymbol{x}}_{0:T}, \bar{\boldsymbol{u}}_{0:T}$ we get the following linear system:

$$\begin{aligned} \delta\boldsymbol{x}_{t+1} &= \boldsymbol{A}_t\delta\boldsymbol{x}_t + \boldsymbol{B}_t\delta\boldsymbol{u}_t + \boldsymbol{G}_t\boldsymbol{\xi}_t \\ \delta\boldsymbol{y}_t &= \boldsymbol{C}_t\delta\boldsymbol{x}_t + \boldsymbol{\eta}_t \end{aligned} \quad (15)$$

Together with a quadratic cost $C_{\text{fb}}$, this forms a LQG problem that can allow us to compute a feedback control to correct for task-relevant errors in a locally optimal fashion.

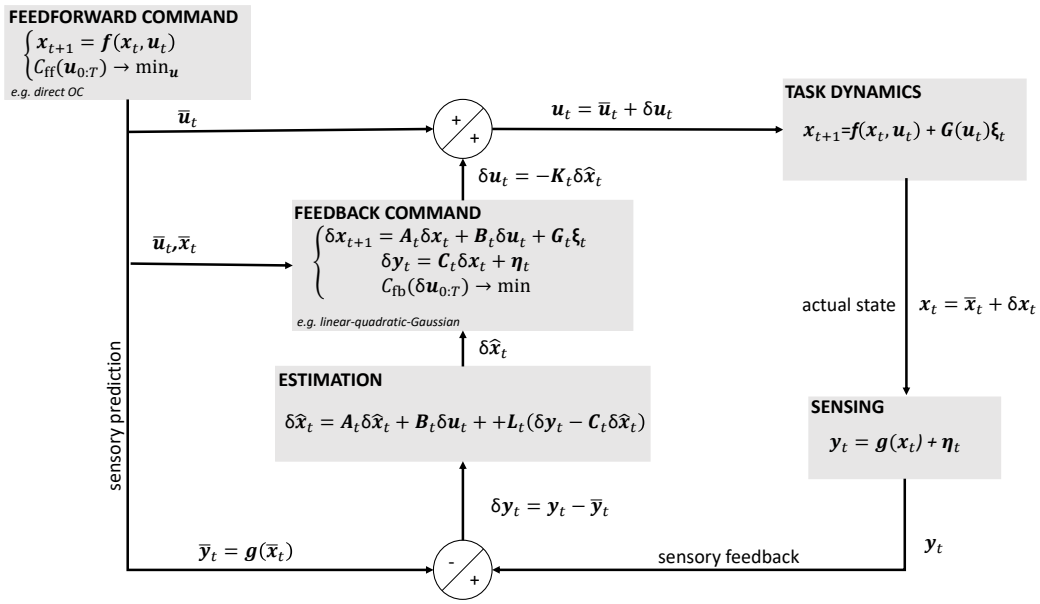


Fig. 2. Scheme for our OC method to generate synthetic humanlike trajectories.The feedforward command is determined with the deterministic OC method introduced in section II.D.1). The feedback command with a LQG corrector is then considered to simulate how humans handle corrections when sensorimotor noise affects their movement as detailed in section II.D.2).

A suitable quadratic cost function can be defined as:

$$C_{\text{fb}}(\delta \boldsymbol{u}_{0:T}) = \mathbb{E}\left[\delta \boldsymbol{x}_T^\top \boldsymbol{Q}\, \delta \boldsymbol{x}_T + \sum_{t=0}^{T} \delta \boldsymbol{u}_t^\top \delta \boldsymbol{u}_t\right] \tag{16}$$

We set $\boldsymbol{Q} = \rho\,\text{diag}(1,1,0,0,0,0)$ as in [24], meaning that we only penalize the final arm posture in (16). Here, $\rho$ is a parameter used to penalize more or less final accuracy, which can affect the optimal feedback gain $\boldsymbol{K}_t$ [34]. Because $C_{\text{fb}}$ also minimizes control-level effort, it ensures that corrections will adhere to the minimum intervention principle, an important hallmark of human motor control [23].

Regarding the output equation, we assume that the complete state, encompassing position, velocity, torque and torque change, can be measured through the integration of multisensory information as in [24], meaning that we simply set $\boldsymbol{g}(\boldsymbol{x}) = \boldsymbol{x}$ so that $\boldsymbol{C} = \boldsymbol{I}_8$. Optimal state estimation $\hat{\boldsymbol{x}}_t$ is achieved using a Kalman filter with optimal gain denoted by $\boldsymbol{L}_t$. The solution used for this LQG problem can be found in [34] for instance (note that the full solution with true multiplicative noise is considered there, which could be integrated into our framework).

A summary of our approximate stochastic OC method used to generate humanlike trajectories (i.e. mean trajectory and its variability across repetitions of the same task) is given in Fig. 2. Timing variability was generated post simulation; trajectories were temporarily remaped to follow a Gaussian distribution of movement duration with the mean as the optimally found timing in the direct OC optimization and a standard deviation set as a 10th of this mean value. This leads to higher variability than observed in humans but leads to better result in average prediction error across subjects as it encompasses more timing preferences.

In practice, the variability of the trajectories can be changed by adjusting on $\boldsymbol{\sigma}, \boldsymbol{\lambda}$, and $\rho$. Here these parameters were adjusted manually to match the variability of another dataset of reaching movements, different from the one used to evaluate the method. In general, these parameters could be user-specific and our method could benefit from a more precise tuning by using few demonstrations. We chose not to do so as it would hinder one of the goals of our approach which is to build a method that is readily usable with no demonstrations and to test it.

## III. Results

In this section we first present the actual and artificial dataset of arm trajectories, and give examples of trajectory inferences. Then we present the prediction accuracy of the data-driven method and our hybrid method for different horizon lengths. The predictive capacity of the data-driven method (ProMPs) was tested with conditioning of the last point (for a new target scenario). We chose to compare our method with the data-driven method with last point conditioning because our method is also informed of the target's center.

### A. Experimental and Artificial Datasets

In Fig. 3, we present a typical example of the movements in the para-sagittal plane gathered during the experimental phase (in this case 10 movements for target 2 by subject #1 of mean duration 1.94sec). Fig. 4 presents the corresponding artificial dataset generated with our method. We generated 1000 movements for every target with an average duration of 1.86sec for target 2.

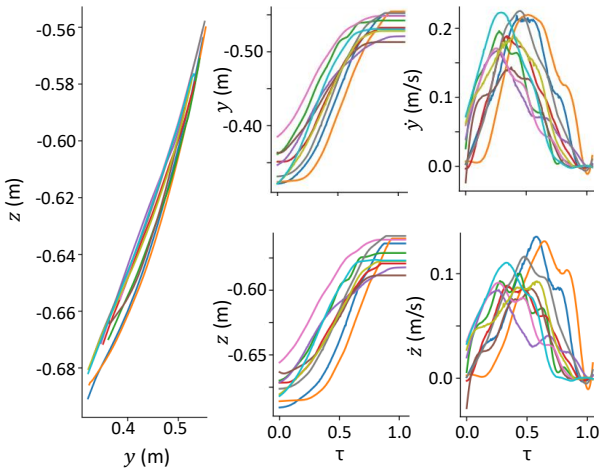


Fig. 3. Experimental movements recorded for target 2 and subject 1. Each color is a single trial.

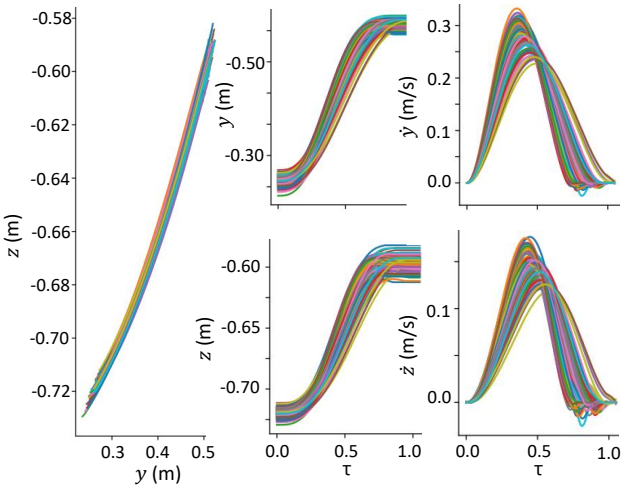


Fig. 4. Artificial movements generated by our optimal control method for target 2. The number of movements generated can be arbitrarily chosen, we chose to simulate 1,000 movements for each target.

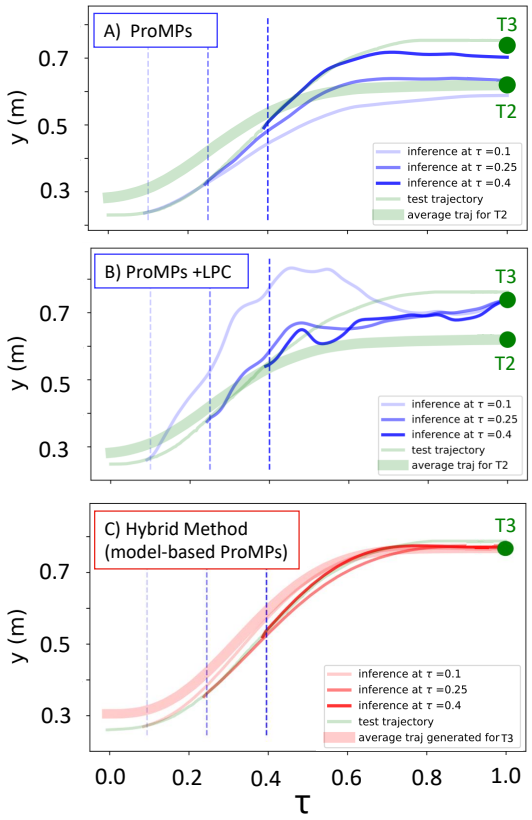


Fig. 5. Examples of successive prediction for the prediction methods. The test trajectory is in green. A) Inferences (in blue) with ProMPs when predicting a trajectory with a different target to the one demonstrated in the training data set (mean trajectory of the learned ProMPs distribution in thick green) At normalized time $\tau$ (successively set to 0.1, 0.25 and 0.4) the ProMPs distribution trained with a dataset of reaching movement for target 2 is conditioned with the observation of the beginning of a movement aiming in reality at target 3. The mean of this conditioned distribution is then used to infer the rest of the trajectory. Note that target 3 is not accurately attained at the end. B) Similar figure where the ProMPs distribution is also conditioned with the center of target 3 as final point. Note that target 3 is now attained but the smoothness of trajectories is much degraded. C) Inferences (in red) with our hybrid method. At normalized time $\tau$ the artificial ProMPs distribution trained with the dataset generated with our model-based approach is conditioned with the observation of the beginning of an experimentally measured movement. The mean of this conditioned distribution is then used as inference. Note that the target is accurately attained and the trajectory remains smooth and close to the test trajectory.

### B. *Inference error results*

Fig. 5 shows typical examples of inferences of a trajectory when predicting movements toward an undemonstrated target. To evaluate each method's accuracy we computed the error for all targets and subjects. Fig. 6 show error graphs for target 2 with mean and standard deviation. A non-null error at the end of the trajectory is observed in Fig. 6 panel B) because in this case predictions are conditioned to reach the new target's center and not the final point of the current test trajectory. As expected, the accuracy of predictions decreases when the distance between the target of the learned dataset and the new target increases.

Fig. 7 shows that the proposed hybrid method outperforms the pure data-driven method on every target except for the one that was used to train the ProMPs. The hybrid method could be further improved by tuning the parameters $\boldsymbol{\sigma}$ and $\boldsymbol{\lambda}$. In this paper, however, their value was fixed as their tuning was achieved from an independent dataset. The accuracy of predictions of our method matches that found in the literature where effective assistance control laws have been developed using predictions with the accuracy equal to $2.22 \pm 1.62$ cm [16].

## IV. Conclusion

We have shown that the proposed hybrid method successfully combines advantages of state-of-the-art model-based and data-driven methods for predicting human movements. On the one hand, it is computationally efficient and can be implemented for the real time control of robotics systems since it readily exploits the ProMPs framework [15]. On the

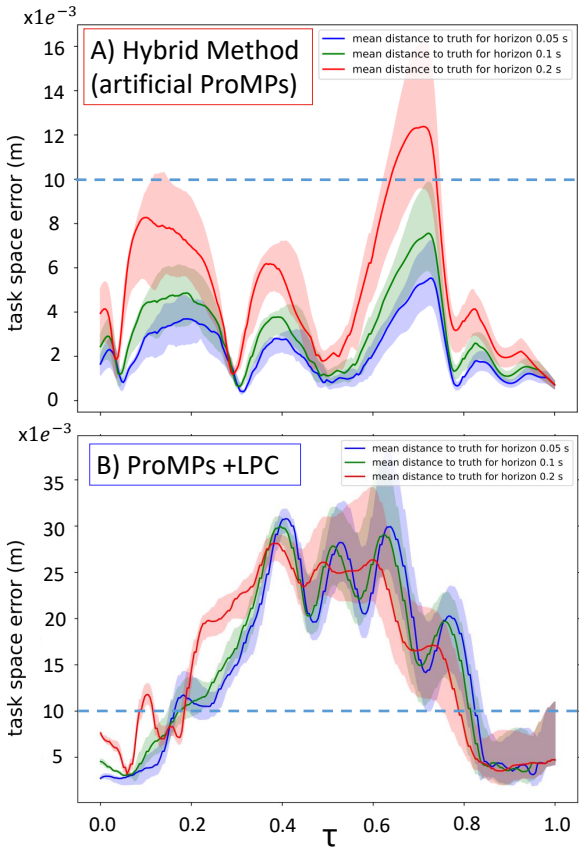


Fig. 6. Task space prediction error, as defined by Eq. 1, along the trajectory for different horizon lengths for target n°2. Mean error in plain line and the shaded area represents the mean standard deviation across different the different trials of the dataset. Blue dotted line at 1cm for scale reference. A) For our hybrid method. Note that the peaks of errors correspond to the moments of acceleration and deceleration. B) For the data-driven method with last point conditioning.

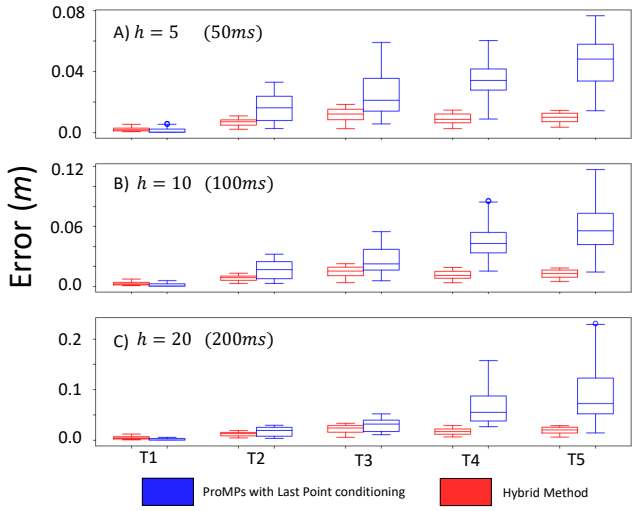


Fig. 7. Boxplots of mean error between prediction and truth when predicting with a ProMPs distribution trained for Target 1 in blue boxplots and conditioned to reach the correct target (Data Based DB with last point conditioning LPC) compared to predictions with a ProMPs distribution trained with artificial data in red boxplots (Model Based MB). Cartesian distance to target 1 for targets 2 to 5 are respectively 0.15m, 0.32m, 0.54m and 0.73m.

other hand, it avoids the need for numerous real demonstrations since it can generate a bunch of artificial demonstrations with the stochastic optimal control framework, to train the ProMPs.

By using a model of human behavior that is taken from the motor control literature [24], we were able to generate a large dataset of humanlike trajectories, including their variability, to a variety of targets. Importantly, these computations can be performed offline. Then, we used these synthetic data to train the ProMPs and predict trajectories in real time on a finite-time receding horizon [16]. This original combination allowed us to accurately predict human movements even in scenarios where no real demonstration is available. Hence, the proposed method requires virtually no training data. Despite the absence of demonstrations, the hybrid method provides predictions with lower spatial errors than the ProMPs when generalization comes into play. Of course, when extensive human data are available for the tasks under consideration, directly using the ProMPs would lead to better results. Our method specifically aims at providing an alternative to avoid the need for such a time-consuming data acquisition stage before assistance can be provided to the user. Extension of our method to higher dimensions and more complex upper limb movements would be possible as the tools are generic but this remains to be tested in future works. Additionally, recent improvements of ProMPs such as [35] could also be implemented into our method as the online usage consists in classical ProMPs use.

With respect to the design of assistive control laws, we plan to combine our prediction method with an active assistance so as to evaluate its impact on the users' comfort and their overall motor behavior. Furthermore, we plan to include the representation of human movement variability provided by the ProMPs as an adaptation factor for the controller. This could allow to maximize the benefits of the assistance, for instance by increasing the exoskeleton's work when the movement's variability is low because predictions are more "trustworthy". Conversely, one could reduce the assistance in high-variability regions resulting in augmenting the robot compliance and avoid non-cooperative scenarios in these regions. Initially, the flow controller of [16] should be tested to compare performance to the literature.

Finally, we plan to analyze if individualising the free parameters of our method (cost functions weights and noise magnitudes) can improve the quality of the predictions. A numerical inverse optimal control approach would be used for this purpose, and a few demonstrations would be required to do so. Indeed, it is known that individuals have usually distinct motor preferences which can be taken into account in cost functions [21], [36]. Hence, personalizing them could result in more symbiotic interaction. This work could also allow us to determine the minimal number of demonstrations per user that are needed to extract their preferred motor

strategy.

## REFERENCES


[1] T. Proietti, V. Crocher, A. Roby-Brami and N. Jarrassé, "Upper-Limb Robotic Exoskeletons for Neurorehabilitation: A Review on Control Strategies," in IEEE Reviews in *Biomedical Engineering*, vol. 9, pp. 4-14, 2016, doi: 10.1109/RBME.2016.2552201.

[2] M. A. Nussbaum, B. D. Lowe, M. de Looze, C. Harris-Adamson, and M. Smets, "An introduction to the special issue on occupational exoskeletons," *IISE Transactions on Occupational Ergonomics and Human Factors*, vol. 7, pp. 153–162, oct 2019.

[3] Y. Li, A. Sena, Z. Wang, X. Xing, J. Babič, E. van Asseldonk, and E. Burdet, "A review on interaction control for contact robots through intent detection," *Progress in Biomedical Engineering*, vol. 4, p. 032004, jul 2022.

[4] D. Verdel, O. Bruneau, G. Sahm, N. Vignais, and B. Berret, "The value of time in the invigoration of human movements when interacting with a robotic exoskeleton," *Science Advances*, vol. 9, sep 2023.

[5] C. Huang, Y. Xiao, and G. Xu, "Predicting human intention-behavior through EEG signal analysis using multi-scale CNN," *IEEE/ACM Transactions on Computational Biology and Bioinformatics*, vol. 18, pp. 1722– 1729, sep 2021

[6] E. Trigili, L. Grazi, S. Crea, A. Accogli, J. Carpaneto, S. Micera, N. Vitiello, and A. Panarese, "Detection of movement onset using EMG signals for upper-limb exoskeletons in reaching tasks," *Journal of NeuroEngineering and Rehabilitation*, vol. 16, mar 2019.

[7] H. Admoni and S. Srinivasa, "Predicting user intent through eye gaze for shared autonomy," in *2016 AAAI Fall Symposium Series*, 2016.

[8] T. Teramae, T. Noda, and J. Morimoto, "EMG-based model predictive control for physical human–robot interaction: application for assist-as-needed control," *IEEE Robotics and Automation Letters*, vol. 3, pp. 210–217, jan 2018

[9] A. Hafs, D. Verdel, W. Gomes, O. Bruneau, and B. Berret, "Optimizing human-robot interactions through differential game control," in *Workshop on Multilimb Coordination in Human Neuroscience and Robotics: Classical and Learning Perspectives*, IROS, Oct. 2023.

[10] L. Bi, A. g. Feleke, and C. Guan, "A review on EMG-based motor intention prediction of continuous human upper limb motion for human-robot collaboration," *Biomedical Signal Processing and Control*, vol. 51, pp. 113–127, may 2019.

[11] L. Quesada, D. Verdel, O. Bruneau, B. Berret, M. A. Amorim, and N. Vignais, EMG-to-torque models for exoskeleton assistance: a framework for the evaluation of in situ calibration. bioRxiv, jan 2024.

[12] S. Calinon, F. D'halluin, E. Sauser, D. Caldwell, and A. Billard, "Learning and reproduction of gestures by imitation," *IEEE Robotics & Automation Magazine*, vol. 17, pp. 44–54, jun 2010.

[13] S. Schaal, S. Kotosaka, and D. Sternad, "Nonlinear dynamical systems as movement primitives," in Humanoids 2000, *First IEEE-RAS International Conference on Humanoid Robots*, CD-Proceedings, 2000.

[14] R. Luo, R. Hayne, and D. Berenson, "Unsupervised early prediction of human reaching for human–robot collaboration in shared workspaces," *Autonomous Robots*, vol. 42, pp. 631–648, jul 2017.

[15] A. Paraschos, C. Daniel, J. R. Peters, and G. Neumann, "Probabilistic movement primitives," *Advances in neural information processing systems*, vol. 26, 2013.

[16] M. Jamsek, T. Kunavar, U. Bobek, E. Rueckert, and J. Babic, "Predictive exoskeleton control for arm-motion augmentation based on probabilistic movement primitives combined with a flow controller," *IEEE Robotics and Automation Letters*, vol. 6, pp. 4417–4424, jul 2021.

[17] Y. Uno, M. Kawato, and R. Suzuki, "Formation and control of optimal trajectory in human multijoint arm movement," *Biological Cybernetics*, vol. 61, pp. 89–101, jun 1989.

[18] T. Flash and N. Hogan, "The coordination of arm movements: an experimentally confirmed mathematical model," *The Journal of Neuroscience*, vol. 5, pp. 1688–1703, jul 1985.

[19] C. M. Harris and D. M. Wolpert, "Signal-dependent noise determines motor planning," *Nature*, vol. 394, pp. 780–784, aug 1998.

[20] B. Berret and F. Jean, "Why Don't We Move Slower? The Value of Time in the Neural Control of Action", *Journal of Neuroscience*, vol. 36, pp. 1056–1070, Jan. 2016.

[21] B. Berret, E. Chiovetto, F. Nori, and T. Pozzo, "Evidence for composite cost functions in arm movement planning: an inverse optimal control approach," *PLoS Computational Biology*, vol. 7, no. 10, pp. 1–18, 2011.

[22] R. J. van Beers, P. Haggard, and D. M. Wolpert, "The role of execution noise in movement variability," *Journal of Neurophysiology*, vol. 91, pp. 1050–1063, feb 2004.

[23] E. Todorov and M. I. Jordan, "Optimal feedback control as a theory of motor coordination," *Nature Neuroscience*, vol. 5, pp. 1226–1235, nov 2002.

[24] B. Berret, A. Conessa, N. Schweighofer, and E. Burdet, "Stochastic optimal feedforward-feedback control determines timing and variability of arm movements with or without vision," *PLOS Computational Biology*, vol. 17, p. e1009047, jun 2021.

[25] D. Verdel, A. Farr, T. Devienne, N. Vignais, B. Berret, and O. Bruneau, "Human movement modifications induced by different levels of transparency of an active upper limb exoskeleton," *Frontiers in Robotics and AI*, vol. 11, Jan. 2024.

[26] P. Garrec, J. P. Friconneau, Y. Measson, and Y. Perrot, 'ABLE, an innovative transparent exoskeleton for the upper-limb', in 2008 IEEE/RSJ *International Conference on Intelligent Robots and Systems*, Nice: IEEE, Sep. 2008, pp. 1483–1488. doi: 10.1109/IROS.2008.4651012.

[27] P. Garrec, 'Screw and cable acutators (SCS) and their applications to force feedback teleoperation, exoskeleton and anthropomorphic robotics.' *Robotics 2010 Curr. Future Challenges*, 167–191. 2010, doi:10.5772/7327

[28] N. Jarrasse and G. Morel, "Connecting a Human Limb to an Exoskeleton," in *IEEE Transactions on Robotics*, vol. 28, no. 3, pp. 697-709, June 2012, doi: 10.1109/TRO.2011.2178151

[29] D. Verdel, G. Sahm, S. Bastide, O. Bruneau, B. Berret and N. Vignais, "Influence of the Physical Interface on the Quality of Human–Exoskeleton Interaction," in *IEEE Transactions on Human-Machine Systems*, vol. 53, no. 1, pp. 44-53, Feb. 2023, doi: 10.1109/THMS.2022.3175415.

[30] Joel A E Andersson , Joris Gillis , Greg Horn , James B Rawlings and Moritz Diehl, 'CasADi – A software framework for nonlinear optimization and optimal control', *Mathematical Programming Computation*, In Press, 2018.

[31] A. Wächter and L. T. Biegler, 'On the implementation of an interior-point filter line-search algorithm for large-scale nonlinear programming', *Math. Program.*, vol. 106, no. 1, pp. 25–57, Mar. 2006, doi: 10.1007/s10107-004-0559-y.

[32] T. Flash and N. Hogan, 'The coordination of arm movements: an experimentally confirmed mathematical model', *J. Neurosci.*, vol. 5, no. 7, pp. 1688–1703, Jul. 1985, doi: 10.1523/JNEUROSCI.05-07-01688.1985.

[33] Coralia Cartis, Jan Fiala, Benjamin Marteau and Lindon Roberts, Improving the Flexibility and Robustness of Model-Based Derivative-Free Optimization Solvers, *ACM Transactions on Mathematical Software*, 45:3 (2019), pp. 32:1-32:41 [arXiv preprint: 1804.00154]

[34] E. Todorov, 'Stochastic Optimal Control and Estimation Methods Adapted to the Noise Characteristics of the Sensorimotor System', *Neural Computation*, vol. 17, no. 5, pp. 1084–1108, May 2005, doi: 10.1162/0899766053491887.

[35] Dermy, Oriane, François Charpillet, and Serena Ivaldi."Multi-modal intention prediction with probabilistic movement primitives." Human Friendly Robotics: 10th International Workshop. *Springer International Publishing*, 2019.

[36] S. Bastide, N. Vignais, F. Geffard and B. Berret, "Interacting with a "Transparent" Upper-Limb Exoskeleton: A Human Motor Control Approach," 2018 IEEE/RSJ International Conference on Intelligent Robots and Systems (IROS), Madrid, Spain, 2018, pp. 4661-4666, doi: 10.1109/IROS.2018.8593991.